INVESTIGATION OF LIPOFUSCIN PHOTOOXIDATION EXTENT USING VISIBLE SPECTROSCOPY AND FLUORESCENCE LIFETIME IMAGING MICROSCOPY

Morozov P.V.[1,2], **Andreev V.S.**[1,2,3], **Tokarev M.A.**[1], **Yakovleva M.A.**[4,5], **Kostyukov A.A.**[4,5], **Feldman T.B.**[4,5], **Kuzmin V.A.**[4], **Ostrovsky M.A.**[4,5], **Goltsman G.N.**[1,3]
[1]Moscow Pedagogical State University, Moscow, Russia
[2]LLC "Supconductor Nanotehnology", Moscow, Russia
[3]National Research University Higher School of Economics, Moscow, Russia
[4]N.M. Emanuel Institute of Biochemical Physics RAS, Moscow, Russia
[5]M.V. Lomonosov Moscow State University, Moscow, Russia

Abstract

The study is devoted to the development of an early preclinical method for the diagnosis of age-related macular degeneration using time-correlated fluorescence microscopy and visible spectroscopy data for the analysis of fluorescence lifetimes and spectra for lipofuscin granules. Lipofuscin granules were obtained from cells of the retinal pigment epithelium of human cadaveric eyes without signs of pathology. To research the fluorescence lifetimes of lipofuscin granules we used the fluorescence excitation method with time-correlated single photon counting technique and the fluorescence lifetimes imaging microscopy (FLIM) method in combination with a superconducting single-photon detector. Photo-oxidized granules were used as a model of age-related macular degeneration. A comparative analysis of the fluorescence lifetimes and spectra before and after photooxidation of lipofuscin granules showed significant differences in the characteristic lifetimes, as well as a shift of the maximum of the fluorescence spectrum to the short-wavelength region. Analysis of the obtained data confirms the possibility of developing a comprehensive method for the spectral and lifetime characterization of fundus autofluorescence. It is necessary to take into account the changes in the contribution of the τ_2 and τ_3 components of the decomposition of the lifetimes curve of fluorescence decay with the longest characteristic lifetime and the shift in the peak of the fluorescence spectrum. This approach will make it possible to determine diagnostic criteria for norm and pathology in the diagnosis of degenerative diseases of the retina and retinal pigment epithelium. Analysis of the data obtained showed that the FLIM method might become promising for the development of an early preclinical method for the diagnosis of age-related macular degeneration of the retina.

Keywords: lipofuscin granule FLIM, fundus autofluorescence (FAF), bisretinoid, fluorescence lifetime, SSPD.

Contacts: Morozov P.V., e-mail: 1pavelmorozov@mail.ru

For citations: Morozov P.V., Andreev V.S., Tokarev M.A., Yakovleva M.A., Kostyukov A.A., Feldman T.B., Kuzmin V.A., Ostrovsky M.A., Goltsman G.N. Investigation of lipofuscin photooxidation extent using visible spectroscopy and fluorescence lifetime imaging microscopy, *Biomedical Photonics*, 2026, vol. 15, no. 2, pp. 18–26. doi: 10.24931/2413–9432–2026–15-2-18-26

ИССЛЕДОВАНИЕ СТЕПЕНИ ФОТООКИСЛЕНИЯ ЛИПОФУСЦИНА МЕТОДАМИ ВИДИМОЙ СПЕКТРОСКОПИИ И ВРЕМЯ-КОРРЕЛИРОВАННОЙ ФЛУОРЕСЦЕНТНОЙ МИКРОСКОПИИ

П.В. Морозов[1,2], **В.С. Андреев**[1,2,3], **М.А. Токарев**[1], **М.А. Яковлева**[4,5], **А.А. Костюков**[4,5], **Т.Б. Фельдман**[4,5], **В.А. Кузьмин**[4], **М.А. Островский**[4,5], **Г.Н. Гольцман**[1,3]
[1]Московский Педагогический Государственный Университет, Москва, Россия
[2]ООО «Сверхпроводниковые нанотехнологии», Москва, Россия
[3]Национальный Университет Высшая Школа Экономики, Москва, Россия
[4]Институт биохимической физики имени Н.М. Эмануэля РАН, Москва, Россия
[5]Московский государственный университет имени М.В. Ломоносова, Москва, Россия

Резюме

Исследование посвящено разработке раннего доклинического метода диагностики возрастной макулярной дегенерации с использованием данных время-коррелированной флуоресцентной микроскопии и видимой спектроскопии при анализе кинетик затухания и спектров флуоресценции для липофусциновых гранул. Липофусциновые гранулы были получены из клеток ретинального пигментного эпителия кадаверных глаз человека без признаков патологии. Для изучения кинетики затухания флуоресценции липофусциновых гранул использовали метод возбуждения флуоресценции с усредненной по образцу корреляцией по времени и метод время-разрешенной флуоресцентной визуализированной микроскопии (FLIM) в сочетании со сверхпроводниковым однофотонным детектором. В качестве модели возрастной макулярной дегенерации использовали фотоокисленные гранулы. Сравнительный анализ кинетик затухания и спектров флуоресценции до и после фотоокисления липофусциновых гранул показал достоверные различия характерных времен жизни, а также смещение максимума спектра флуоресценции в коротковолновую область по мере окисления образцов. Полученные данные позволяют сделать вывод о том, что для разработки метода спектрально-кинетического анализа аутофлуоресценции глазного дна необходимо учитывать изменение вклада τ_2 и τ_3 компонент разложения кинетической кривой затухания флуоресценции τ_m с наибольшим характерным временем жизни и смещение пика спектра флуоресценции. Такой подход позволит определить диагностические критерии для нормы и патологии при диагностике дегенеративных заболеваний сетчатки и ретинального пигментного эпителия. Анализ полученных данных показал, что метод FLIM, может стать перспективным для разработки раннего доклинического метода диагностики возрастной макулярной дегенерации сетчатки.

Ключевые слова: липофусциновая гранула, FLIM, аутофлуоресценция глазного дна (FAF), бисретиноид, кинетика затухания флуоресценции, SSPD.

Контакты: Морозов П.В., e-mail: 1pavelmorozov@mail.ru

Для цитирования: Морозов П.В., Андреев В.С., Токарев М.А., Яковлева М.А., Костюков А.А., Фельдман Т.Б., Кузьмин В.А., Островский М.А., Гольцман Г.Н. Исследование степени фотоокисления липофусцина методами видимой спектроскопии и время-коррелированной флуоресцентной микроскопии // Biomedical Photonics. – 2026. –Т. 15, № 2. – С. 18–26. doi: 10.24931/2413–9432–2026–15-2-18-26

Introduction

One of the most common causes of vision loss in the elderly is age-related macular degeneration (AMD) [1]. The development of AMD is accompanied by pathological changes in the retinal pigment epithelium (RPE) and, ultimately, by the death of retinal photoreceptor cells [1, 2]. Currently, the disease is considered practically incurable; therefore, an important task is the earliest possible detection of AMD with the aim of taking timely protective and preventive measures that can slow the progression of this severe ocular pathology and preserve vision and a good quality of life for the patient for many years. In this regard, particular attention is paid to the development of methods for early, preclinical diagnosis of degenerative diseases of the retina and RPE, in particular, the improvement and expansion of the diagnostic capabilities of the existing modern non-invasive diagnostic method – fundus autofluorescence [3, 4]. This method makes it possible to study pathological areas of the fundus in considerable detail when investigating, for example, early manifestations of AMD and its progression. The method of recording fundus autofluorescence allows one to assess the state of RPE cells in patients with AMD, choose a treatment strategy, and make a prognosis regarding the development of the disease. It is one of the most sensitive modern methods for studying early changes in the retina/RPE complex [5], which provides an opportunity for the prevention of early stages of the disease, as well as for qualitative objective assessment of treatment effectiveness.

The autofluorescence method is based on obtaining an image created mainly by the intrinsic fluorescence of the so-called "age pigment" – lipofuscin granules (LG), which are formed and accumulate in RPE cells as a result of incomplete lysosomal degradation of phagocytosed photoreceptor cell debris during aging and especially intensely during the development of degenerative diseases of the retina and RPE [6]. The fluorescent properties of LG are mainly determined by the presence in them of conjugates of all-trans retinal, the so-called bisretinoids – bis-retinylidene-ethanolamine (A2E) [7] and other compounds, as well as products of their photooxidation and photodegradation (oxidized bisretinoids) [8].

LG are photosensitive and, upon absorption of light in the visible spectral region, contribute to the formation of reactive oxygen species (ROS) [9]. The source of ROS in LG are bisretinoids. In this case, the bisretinoids themselves are readily oxidized upon interaction with ROS to form oxidized bisretinoids. The fluorescence spectrum of these products shifts to the short-wavelength region [10]. Oxidized bisretinoids are extremely toxic; accumulating in RPE cells, they are capable of damaging vital cellular structures even in the absence of light [11].

It was previously shown that in AMD, an increased content of oxidized bisretinoids is observed compared to the norm [12]. Therefore, the change in fluorescence spectra caused by an increase in the content of oxidized bisretinoids can be considered a diagnostic sign of the early preclinical stage of the disease [13]. Intensive attempts are currently being made to improve the non-invasive diagnostic method of fundus autofluorescence [14]. It is quite obvious that the qualitative and quantitative recording of LG fluorescent characteristics (fluorescence spectra,

fluorescence decay kinetics) can serve as an important prognostic criterion for the development of degenerative diseases of the retina. Experiments on studying the fluorescence decay kinetics of LG using time-correlated single-photon counting have been conducted [12, 15]. The research results showed that oxidized bisretinoids have the longest characteristic fluorescence lifetimes compared to non-oxidized bisretinoids. This result allowed explaining the phenomenon of increased mean fluorescence lifetime in AMD [16, 17]. In other words, an increased content of oxidized bisretinoids in LG of RPE cells leads to an increase in the mean fluorescence lifetime in pathology [13]. However, it should be noted that in the works of Feldman T.B. *et al.* [12] and Yakovleva M.A. *et al.* [15], averaged data of characteristic lifetimes were obtained when studying samples of RPE cell suspension or chloroform extract of LG.

A limitation of the classical method is that it is one-dimensional and does not transmit an image directly, nor can it be used in combination with fast scanning used in modern laser scanning microscopes [18]. To confirm these conclusions, experiments using fluorescence lifetime imaging microscopy (FLIM) are necessary. This method allows obtaining higher accuracy of lifetime or photon registration efficiency at a given number of photons detected from the sample [19], and the result of lifetime measurement does not depend on the concentration of fluorophores and variations in absorption in the studied sample [20]. Using the FLIM method, it is possible to analyze the spatial distribution of characteristic lifetimes in a LG sample before and after their photooxidation.

Simultaneous measurement of decay kinetics and fluorescence spectra of LG provides more data for analysis and, consequently, for improving the method of early diagnosis of eye diseases.

Thus, the aim of this work was a comparative analysis of the fluorescence decay kinetics of individual LGs obtained from RPE of human cadaveric eyes before and after photooxidation, using the FLIM method based on a laser galvanometer scanner and a superconducting single-photon detector (SSPD/SNSPD), with simultaneous measurement of LG fluorescence spectra. In addition, the aim of the research was to visualize the spatial distribution of LG fluorescence lifetimes by the FLIM method to determine the contributions of bisretinoids and oxidized bisretinoids to the overall fluorescence kinetics.

Materials and Methods

Object - Lipofuscin Granules

Human cadaveric eyes were obtained from the Federal State Autonomous Institution "National Medical Research Center "Microsurgery of the Eye" named after Academician S.N. Fedorov" from more than 100 donors in the age group 50-75 years without signs of pathology, from the thanatology departments of the Moscow Bureau of Forensic Medical Examination [10], according to the method described in the work of Boulton M. *et al.* [9]. Human cadaveric eyes were obtained within 10 hours after donor death after removal of the cornea for transplantation. Each cadaveric eye was carefully examined by an ophthalmologist. Analysis and screening selection of donor material were carried out according to clinical signs. The study of samples was carried out under subdued lighting.

Setup for Simultaneous Measurement of Fluorescence Spectra and Fluorescence Lifetimes

To simultaneously measure fluorescence spectra and fluorescence decay kinetics, a radiation collection scheme from a quartz cuvette placed in a holder was used: optical fibers for radiation collection were installed on two sides of the cuvette, one connected to the SSPD, the signal from which, together with the laser synchronization signal, was connected to a Time Tagger Ultra device for time-correlated counting and measurement of decay kinetics (Swabian, Germany), the second fiber was connected to an ATP5020P spectrometer (OptoSky, China). 500 LP filters (Chroma, USA) were installed in front of the optical fibers to cut off the possibility of laser excitation radiation entering. The sample was irradiated with a laser from the third side – perpendicular to the edges of the cuvette, from which the useful signal was collected. To excite fluorescence, a BDL-472-SMC laser with a wavelength of 473 nm and a picosecond pulse repetition rate of 50 MHz was used; the average laser power did not exceed 57 μW/s. The experimental setup is shown in Fig. 1.

Superconducting Single-Photon Detector

The manufacturing method of the SSPD is described in the article by Smirnov K. *et al.* [21]. The active area of the detector was 15×15 μm^2, and the detector was combined with a single-mode fiber SMF-28e (Corning, USA). The dependence of dark counts and detection system efficiency was measured using an SC-PRO 7 supercontinuum laser [YSL Photonics, China]. The method for measuring the efficiency of the optical system consists of measuring the number of detector counts compared to the incident radiation power on the detector [22]. The measured detection efficiency of the system was more than 60% in a wide wavelength range of 500-950 nm. The main advantages of the SSPD are low dark count rate (up to 0.1 counts/s) [23], low jitter [22], and high quantum efficiency [21].

Visualization of the Spatial Distribution of Fluorescence Lifetimes

During measurements by the FLIM method, a scanning system based on a DCS-120 confocal galvanometer scanner (Becker & Hickl, Germany) with a Zeiss AXIO Observer A1 microscope (Zeiss, Germany), with objectives (x20, x40, x60), and a picosecond diode laser BDL-472-SMC were used; time-correlated counting was performed using an SPC-150NX board. The optical system of the laser confocal galvanometer scanner was modified to interface with the

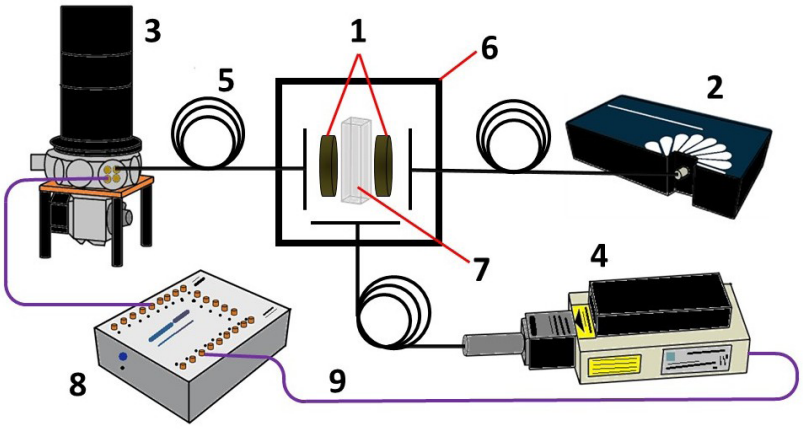

Рис. 1. Схема одновременного измерения спектров флуоресценции и времен жизни флуоресценции: 1 – фильтры (500 LP); 2 – спектрометр, 3 – SSPD криостат; 4 – лазер 473 нм; 5 – оптическое волокно; 6 – черный ящик; 7 – кварцевая кювета с суспензией ЛГ; 8 – время-разрешающая электроника Swabian; 9 – коаксиальный кабель.
Fig. 1. Scheme for simultaneous measurements of fluorescence spectra and lifetimes: 1 – filters (500 LP); 2 – spectrometer; 3 – cryostat with SSPD; 4 – laser 473 nm; 5 – optical fiber; 6 – black Box; 7 – quartz cuvette with suspension of lipofuscin granules; 8 – time tagger Swabian; 9 – coaxial cable.

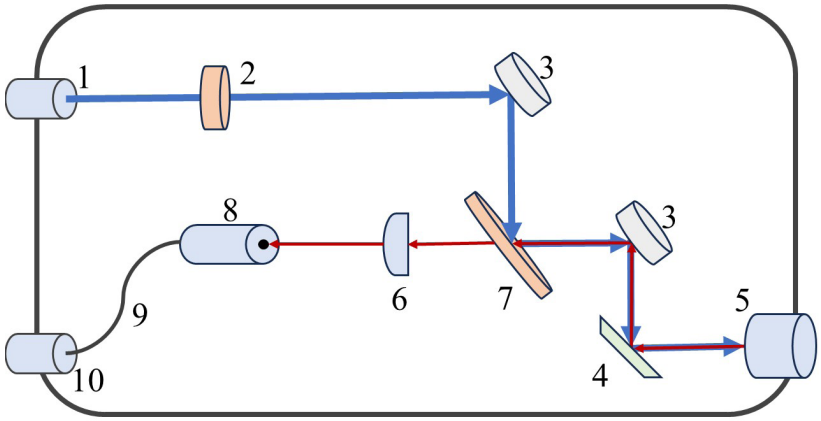

Рис. 2. Оптическая схема установки: 1 – вход лазера; лазерное излучение (синие стрелки); 2 – полосовой фильтр 473+-20 нм; 3 – зеркала; 4 – гальвано-зеркала; 5 – выход на микроскоп, сигнал люминесценции (красные стрелки); 6 – фокусирующая линза; 7 – дихроическое зеркало (500 LP); 8 – коллиматор одномодового оптического волокна; 9 – одномодовое оптическое волокно; 10 – вход на SSPD.
Fig. 2. Optical scanning scheme: 1 – laser In, laser signal (blue arrows); – band pass filter 473+-20 nm; 3 – mirrors; 4 – galvano-mirrors; 5 – to microscope, luminescence signal (red arrows); 6 – focusing lens; 7 – dichroic mirror (500 LP); 8 – SM-fiber coupler; 9 – SM-fiber; 10 – to SSPD.

optical fiber input of a single-photon superconducting detector (Fig. 2) located in an OPRS-SW-70-WB-SMF closed-cycle machine (Scontel, Russia). For FLIM analysis, the LG suspension was applied with a pipette onto the glass of a special bottom Petri dish (Fluorodish, USA) and then placed under the microscope objective, selecting a position with an accumulation of granules in the objective focus.

When measuring the temporal resolution of the entire system, a silver mirror was placed on the objective in the microscope focus. The measurement technique is described in the work of Shcheslavskiy V. *et al*. [22]. The measured temporal resolution (jitter) of the entire system at a wavelength of 473 nm was 76 ps: including the picosecond 473 nm laser (51 ps), the SSPD-based detection system (48 ps), consisting of the detector and electronics, and the SPC-150NX correlation measurement board (2.7 ps).

The laser excitation radiation was directed via the optical scheme to two galvanometer mirrors, which, in turn, performed pixel-by-pixel scanning of the sample in the working plane of the microscope. The fluorescence signal from the LG sample then hit the same mirror system and was redirected via a dichroic mirror to a lens, which focused the signal onto a coupler coupled to the optical fiber input of the detector. A 500 LP long-pass filter (Chroma, USA) was used to register fluorescence in the required range. Using the signal correlation program with pixel scanning, data on the distribution of intensities and fluorescence lifetime components at each point were constructed. The obtained data were processed using the SPCImage program (B&H, Germany).

Photooxidation of Lipofuscin Granules

The LG suspension was placed in a quartz cuvette or in a Petri dish (Fluorodish). LG samples were exposed to a 473 nm laser in CW mode with an average power of 1.5 mW for 1, 3, and 5 minutes. Laser irradiation caused the photooxidation process of LG.

Results

Fluorescent Properties of Lipofuscin Granules Before and After Their Photooxidation

The optical properties of the suspension of native and photooxidized LGs were studied using a setup for simultaneous registration of fluorescence spectra and fluorescence decay kinetics. Fig. 3 presents the fluorescence spectra of LGs; measurements were carried out on an ATP5020P spectrometer (Optosky, China) in the wavelength range of 500-800 nm.

The data in Fig. 3, it follows that upon gradual irradiation with a 473 nm CW laser with an average power of 1.5 mW, the fluorescence spectrum maximum shifts to the short-wavelength region. From the obtained data for photooxidized samples, a redistribution of spectrum intensities in the short-wavelength region of 500-550 nm and in the long-wavelength region of 650-800 nm can be observed. This is due to the oxidation process of LG and the formation of oxidized bis-retinoids, which have a shorter wavelength spectrum compared to the initial sample. It can be seen that in photooxidized LGs, the fluorescence intensity increases in the short-wavelength part of the spectrum and decreases in the long-wavelength part. Spectrum 4 in Fig. 3 reflects the extreme degree of LG photooxidation, after which the spectral shift is no longer observed and does not depend on either irradiation time or laser power – this may indicate that all LGs have transitioned to an oxidized state.

In this work, a detailed, step-by-step study of the dependence of the fluorescence maximum on the LG irradiation time was carried out; Fig. 4 shows a linear dependence of the shift of the fluorescence maximum on the duration of laser irradiation. However, at irradiation times of LG with the laser exceeding 160-170 min, the graph reaches a plateau (Fig. 4), leading to the conclusion of complete photooxidation of the sample.

The spectroscopy data are in good agreement with the results of high-performance liquid chromatography of previous studies [24]; thus, in photooxidized LG samples, there are more oxidized bisretinoids compared to non-oxidized ones. It is the increased content of oxidized bisretinoids in photooxidized LGs that leads to a shift of the fluorescence maximum to the short-wavelength region of the spectrum [9, 11].

Registrarion of Fluorescence Decay Kinetics of Lipofuscin Granules

Measurement of fluorescence lifetimes for the LG suspension was carried out using the time-correlated single-photon counting (TCSPC) method. During the experiment,

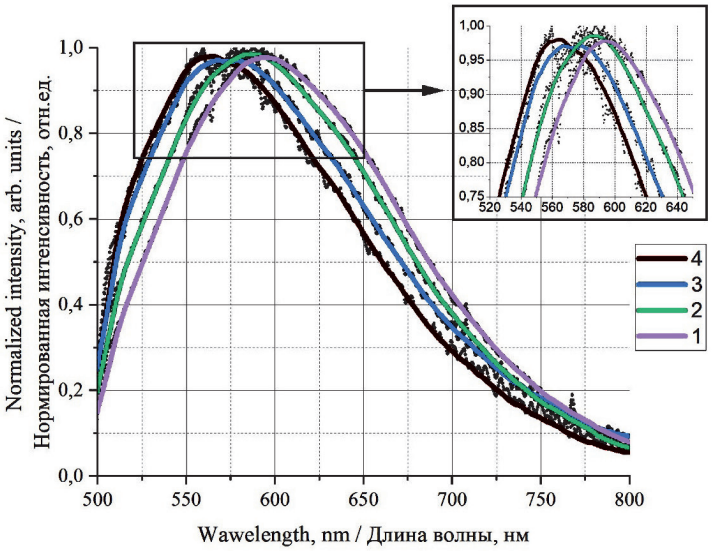

Рис. 3. Нормированные спектры флуоресценции ЛГ в исходном (спектр 1) и фотоокисленном состояниях (спектр 2, 3, 4). Вставка: Увеличенное изображение спектра флуоресценции в области максимума.
Fig. 3. Normalized fluorescence spectra of lipofuscin granules: native (curve 1) and photooxidized (curves 2, 3, 4).
Insert: enlarged image of the fluorescence spectra in the maximum region.

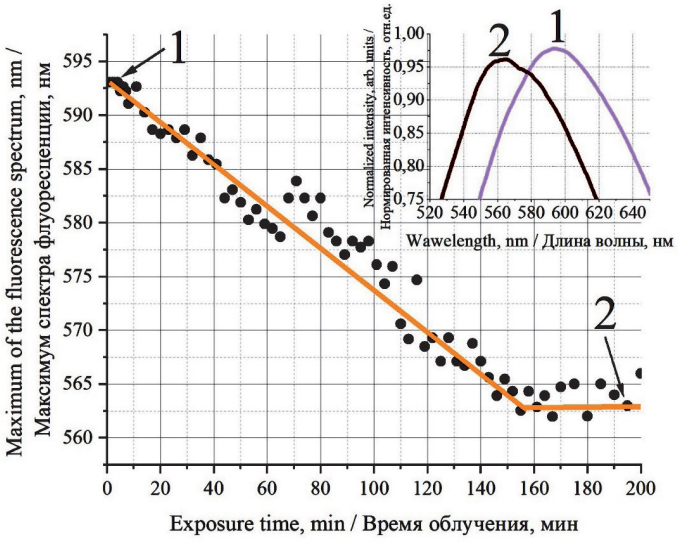

Рис. 4. Смещение максимума в спектрах флуоресценции для суспензии ЛГ от времени облучения CW-лазером (λ_{exc} = 473 нм): кривая 1 – до фотоокисления, кривая 2 – после фотоокисления.
Вставка: Крайние положения максимумов спектра флуоресценци ЛГ: 1 – до облучения, 2 – после облучения и выхода на плато.
Fig. 4. Fluorescence spectra maximum shift of lipofuscin granules in dependence of CW-laser exposition time, (λ_{exc} = 473 nm): curve 1 – native, curve 2 – photooxidized.
Insert: Extreme positions of the fluorescence spectrum maxima of lipofuscin granules: 1 – before irradiation, 2 – after irradiation and reaching a plateau.

the stepwise change in the mean lifetime τ_1 before and after the photooxidation process of LG was recorded. The obtained data are shown in Fig. 5. Signal accumulation using the TCSPC method was carried out for 2 minutes. The excitation laser wavelength was λ_{exc} = 473 nm, with a pulse repetition rate of 50 MHz; fluorescence lifetimes were recorded at wavelengths λ_{reg} >500 nm.

The mean fluorescence lifetime τm was calculated using the formula, within the framework of a three-exponential model [25]:

$$\boldsymbol{\tau}_m = (A_1 \times \tau_1 + A_2 \times \tau_2 + A_3 \times \tau_3)/(A_1 + A_2 + A_3).$$

From Fig. 5, it can be seen that with increasing laser irradiation time, the lifetime for the first component τ1 increases from 226 to 552 ps, which indicates an increase in the content of oxidized bisretinoids in the LG composition, which have a larger proportion of long-lived components $\boldsymbol{\tau}_2$ and $\boldsymbol{\tau}_3$ compared to the non-oxidized sample. Table 1 presents the individual components $\boldsymbol{\tau}_j$ of the fluorescence lifetime decay and the amplitudes ($\mathbf{A}_j$) of each component.

From Table 1, it follows that in photooxidized LGs, the contribution ($\mathbf{A}_3$) of the long-lived component ($\boldsymbol{\tau}_3$) increases, while the contribution of the first component ($\mathbf{A}_1$) with the shortest characteristic time ($\boldsymbol{\tau}_1$) decreases. It is also seen here that the mean fluorescence lifetime ($\boldsymbol{\tau}_m$) increases, which is consistent with literature data [26, 27].

Spatial Distribution of Fluorescence Lifetimes

Using a laser confocal scanner with the FLIM method combined with SSPD, data on the spatial distribution of characteristic fluorescence lifetimes depending on spatial coordinates in samples of native and photooxidized LGs were obtained (Fig. 6).

In contrast to the averaged data obtained from the analysis of fluorescent characteristics for the LG suspension (Fig. 4, Fig. 5), this section presents the results of detailed FLIM imaging of the spatial distribution of characteristic fluorescence lifetimes ($\boldsymbol{\tau}_j$) in LG samples placed on the bottom of a Petri dish (Fluorodish). Such analysis allows for a more detailed study of the lifetime distribution across the LG sample and the creation of a surface lifetime map, and also provides the opportunity to examine individual components of the fluorescence decay kinetic curves in more detail and track changes in the temporal characteristics of LG fluorescence decay during their stepwise photooxidation.

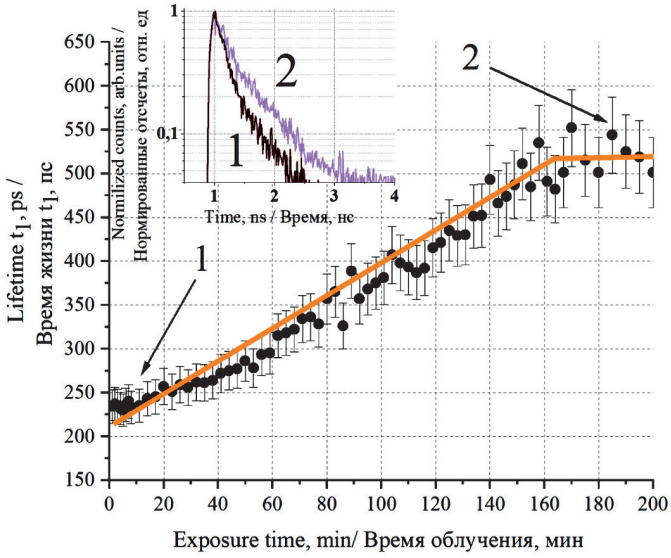

Рис. 5. Зависимость времени жизни первой компоненты флуоресценции τ_1 от времени облучения суспензии ЛГ лазером 473 нм в CW режиме.
Вставка: кинетики затухания флуоресценции для суспензии ЛГ до (кривая затухания 1) и после полного фотоокисления (кривая затухания 2), выхода графика на плато.
Fig. 5. The dependence of the first lifetime τ_1 component of fluorescence on the irradiation time of the suspension of lipofuscin granules with a 473 nm laser in CW mode.
Insert: kinetics of fluorescence lifetimes for a suspension of lipofuscin granules before (curve 1) and after (curve 2) complete photooxidation, the graph reaches a plateau.

Таблица 1
Компоненты разложения τ_j времен жизни флуоресценции для суспензии ЛГ до и после их фотоокисления (λ_{exc} = 473 нм, λ_{reg} > 500 нм), полученные методом TCSPC (из данных рис. 5)

Table 1
Components of the decomposition τ_j of the fluorescence lifetimes for a suspension of lipofuscin granules before and after photooxidation (λ_{exc} = 473 nm, λ_{reg} > 500 nm), obtained by the TCSPC method (from the data of Fig. 5).

Образец Sample	τ_1, пс τ_1, ps	A_1% A_1%	τ_2, пс τ_2, ps	A_2% A_2%	τ_3, пс τ_3, ps	A_3% A_3%	τ_m, пс τ_m, ps	A_2+A_3/A_1 A_2+A_3/A_1
Нативные ЛГ Native LG	226	66	649	27	2012	7	583	0.51
Фотоокисленные ЛГ Photooxidized LG	552	55	1594	31	4106	14	1671	0.82

ЛГ – липофусциновые гранулы, А – амплитуда в % для j-компоненты разложения времени жизни флуоресценции, τ – время жизни флуоресценции для j-компоненты.
LG – lipofuscin granules, A – is the amplitude in % of the j-component of the fluorescence lifetime decomposition, τ – is the fluorescence lifetime for the j-component.

Discussion of Results

Within the framework of the three-exponential model [25], characteristic fluorescence lifetimes were calculated for both experiments based on averaged data obtained by the TCSPC method for the LG suspension (Fig. 5 and Table 1) and the results of FLIM imaging of the spatial distribution of fluorescence lifetimes (Fig. 6, Table 2).

From Table 2, it can be seen that in photooxidized LGs, the contribution of the long-lived component (τ_3) increases, while the contribution of the component (τ_1) with the shortest characteristic time decreases. At the same time, the mean fluorescence lifetime (τ_m) increases, which correlates well with previous studies [15, 26, 27].

Thus, the analysis of fluorescence decay curves of the suspension of native and photooxidized LGs showed that the kinetics of changes in characteristic fluorescence lifetimes obtained on both setups have the same trend: there is an increase in the value of τm, which is the characteristic average lifetime for the fluorescence of oxidized bisretinoids [15, 24], and an increase in the contribution of long-lived (A_2, A_3) components to the fluorescence decay kinetic curve (Tables 1 and 2). Previous studies [15, 24, 26] have shown that it is oxidized bisretinoids that have the longest characteristic fluorescence lifetimes compared to non-oxidized bisretinoids.

A detailed analysis of fluorescence lifetimes for native LGs and photooxidized ones shows that for searching numerical criteria of normal and pathological conditions in diagnostics using the FLIM method, using only averaged values of characteristic fluorescence lifetimes and their contribution to the overall kinetics can lead to incorrect conclusions, since it is known that LG contain more than 20 types of fluorophores [28, 29, 30] and the distribution of τ_1, τ_2, and τ_3 across the LG sample in the Petri dish can vary within a certain range of decay times; if only the mean lifetime τm is taken into account, this valuable diagnostic information is lost.

Since the FLIM method is considered a promising approach for expanding the capabilities of the fundus autofluorescence method [31], it is necessary to define clear criteria for normal and pathological conditions. This concerns not only the fluorescent properties of the object under study itself, but also the methods of recording and determining numerical criteria. Analyzing the obtained data, it can be concluded that determining the exact values of characteristic fluorescence lifetimes for normal and pathological conditions, and especially their averaged values, can cause certain difficulties. Perhaps this is why the FLIM method has not yet been widely introduced into clinical practice.

Conclusion

In this work, a comparative analysis of the fluorescence decay kinetics of native and photooxidized LGs was carried out using two time-resolved fluorescence microscopy methods: the classical (sample-averaged) time-correlated single-photon counting (TCSPC) method and the fluorescence lifetime imaging (FLIM) method using a

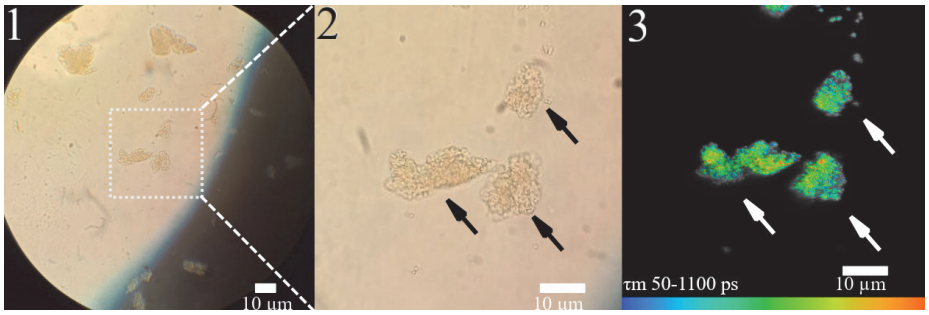

Рис. 6. Изображение ЛГ (1), полученное на микроскопе (объектив 40x, NA 0.8), область сканирования (2) и программно-увеличенное изображение FLIM (3). Разрешение FLIM 512x512 пикс 1024 каналов на пикс.
Fig. 6. Image of lipofuscin granules (1) obtained on a microscope (40x objective NA 0.8), scanning area (2) and programmatically enlarged FLIM image (3). FLIM resolution is 512x512 pixels, 1024 bins per pixel.

Таблица 2
Отдельные компоненты разложения τ_i времен жизни флуоресценции ЛГ до и после их фотоокисления (λ_{exc} = 473 нм, λ_{reg} > 500 нм), полученные методом FLIM (из данных рис. 6 (3))

Table 2
Individual components of decomposition τ_i of the fluorescence lifetimes of lipofuscin granules before and after photooxidation (λ_{exc} = 473 nm, λ_{reg} > 500 nm), obtained by the FLIM method (from the data of Fig. 6(3))

Образец Sample	τ_1, пс τ_1, ps	A_1% A_1%	τ_2, пс τ_2, ps	A_2% A_2%	τ_3, пс τ_3, ps	A_3% A_3%	τ_m, пс τ_m, ps	A_2+A_3/A_1 A_2+A_3/A_1
Нативные ЛГ Native LG	214	68	670	24	2104	8	502	0.47
Фотоокисленные ЛГ Photooxidized LG	567	52	1650	35	4030	13	1412	0.92

ЛГ – липофусциновые гранулы, A – амплитуда в % для j-компоненты разложения времени жизни флуоресценции, τ – время жизни флуоресценции для j-компоненты.
LG – lipofuscin granules, A – is the amplitude in % of the j-component of the fluorescence lifetime decomposition, τ – is the fluorescence lifetime for the j-component.

laser galvanometer scanner for direct measurement of fluorescence with picosecond temporal resolution combined with a superconducting single-photon detector.

Fluorescence analysis and high-performance liquid chromatography [24] showed that irradiation of LG leads to their photooxidation. Photooxidized samples were used as a model of AMD.

The study of fluorescence decay kinetics by two methods on different experimental setups showed good correlation both with each other and with literature data. It was established that during LG photooxidation, there is a change in the contribution of characteristic lifetimes to the overall fluorescence decay kinetics. The contribution with the shortest characteristic time decreases, while the contributions of the intermediate and longest lifetimes increase. This change in parameters occurs due to an increase in the content of oxidized bisretinoids in photooxidized LGs, which, in turn, leads to an increase in the value of the mean fluorescence decay time.

Currently, one of the approaches in the development of spectral methods for analyzing autofluorescence is the measurement of the mean fluorescence decay time using the TCSPC method. It is now beyond doubt that in some visual pathologies, particularly AMD, there is an increase in the mean fluorescence decay time, which allows considering this parameter as a potential criterion for degenerative processes in the retina and RPE during early diagnosis. It should be noted, however, that a universal diagnostic criterion value for normal and pathological conditions has not yet been determined.

FLIM imaging of the spatial distribution of characteristic LG fluorescence lifetimes made it possible to analyze the kinetics of changes in characteristic lifetimes during LG photooxidation across the entire sample surface, in the center and at the periphery (Fig. 6). Considering the fact that the degree of retinoid oxidation in LG can vary, it can be concluded that the FLIM distribution pattern of fluorescence lifetimes will also change. It follows that determining a diagnostic criterion for degenerative processes in the retina and RPE based solely on measuring the mean LG fluorescence decay time τm cannot provide an objective assessment of the degree of pathology progression; changes in fluorescence spectra must be taken into account, as well as the contribution of individual decay components τ_j of fluorescence lifetimes, as was demonstrated in the present study.

This work was supported by grant No. 23-65-10005 from the Russian Science Foundation.

This work was supported by the Ministry of Science and Higher Education of the Russian Federation (project No. 122041400102-9) and as part of a state assignment to Lomonosov Moscow State University.

REFERENCES

1. Rózanowska M.B. Lipofuscin, its origin, properties, and contribution to retinal fluorescence as a potential biomarker of oxidative damage to the retina. *Antioxidants*, 2023, vol. 12, pp. 2111. doi: 10.3390/antiox12122111.
2. Dorey K.C., Wu G., Ebensrein D., Garsd A. Cell loss in the aging retina: relationship to lipofuscin accumulation and macular degeneration. *Invest. Ophthalmol. Vis. Sci*., 1989, vol. 30, pp. 1691–1699. doi: 10.1016/S0161-8105(89)31221-5.
3. Schmitz Valckenberg S., Holz F.G., Fitzke F.W. Perspectives in imaging technologies. In: Holz F.G., Schmitz Valckenberg S., Spaide R.F., Bird A.C. (eds). *Atlas of fundus autofluorescence imaging.* Berlin: Springer, 2007, pp. 331–338. doi: 10.1007/978-3-540-71994-6_19.
4. Sharifzadeh M., Gellermann W. Systems and methods for optical detection of lipofuscin concentration in a subject's eye. *US Patent*, 2011, no. 7,914,147 B2.
5. Holz F.G., Schmitz Valckenberg S., Spaide R.F., Bird A.C. *Autofluorescence imaging.* Berlin, Heidelberg: Springer Verlag, 2007, pp. 342. doi: 10.1007/978-3-540-71994-6.
6. Holz F.G., Schutt F., Kopotz J. Inhibition of lysosomal degradative functions in RPE cells by a retinoid component of lipofuscin. *Invest. Ophthalmol. Vis. Sci*., 1999, vol. 40, pp. 737. PMID: 10067978.
7. Eldred G.E., Lasky M.R. Retinal age pigments generated by self-assembling lysosomotropic detergents. *Nature,* 1993, vol. 361, pp. 724. doi: 10.1038/361724a0.
8. Von Ruckmann A., Fitzke F.W., Bird A.C. In vivo fundus autofluorescence in macular dystrophies. *Arch. Ophthalmol*., 1997, vol. 115, pp. 609–615. doi: 10.1001/archopht.1997.01100150611006.
9. Boulton M., Dontsov A., Jarvis Evans J., Ostrovsky M., Svistunenko D. Lipofuscin is a photoinducible free radical generator. *J. Photochem. Photobiol. B: Biol*., 1993, vol. 19, pp. 201–204. doi: 10.1016/1011-1344(93)07173-3.
10. Yakovleva M.A., Feldman T.B., Krupennikova A.S., Borzenok S.A., Ostrovsky M.A. Fluorofory lipofuscinovych granul, otvetstvennie za autofluorescenciyu glaznogo dna cheloveka. *Izvestiya Akademii Nauk. Seriya Khimicheskaya*, 2010, no. 12, pp. 2252–2260.
11. Sparrow J.R., Vollmer Snarr H.R., Zhou J. et al. A2E epoxides damage DNA in retinal pigment epithelial cells. Vitamin E and other antioxidants inhibit A2E epoxide formation. *J. Biol. Chem*., 2003, vol. 278, no. 20, pp. 18207–18213. doi: 10.1074/jbc.M300155200.

ЛИТЕРАТУРА

1. Rózanowska M.B. Lipofuscin, its origin, properties, and contribution to retinal fluorescence as a potential biomarker of oxidative damage to the retina // Antioxidants. – 2023. – Vol. 12. – P. 2111. doi: 10.3390/antiox12122111.
2. Dorey K.C., Wu G., Ebensrein D., Garsd A. Cell loss in the aging retina: relationship to lipofuscin accumulation and macular degeneration // Invest. Ophthalmol. Vis. Sci. – 1989. – Vol. 30. – P. 1691–1699. doi: 10.1016/S0161-8105(89)31221-5.
3. Schmitz-Valckenberg S., Holz F.G., Fitzke F.W. Perspectives in imaging technologies // In: Holz F.G., Schmitz-Valckenberg S., Spaide R.F., Bird A.C. (Eds). Atlas of fundus autofluorescence imaging. – Berlin: Springer, 2007. – P. 331–338. doi: 10.1007/978-3-540-71994-6_19.
4. Sharifzadeh M., Gellermann W. Systems and methods for optical detection of lipofuscin concentration in a subject's eye // US Patent. – 2011. – No. 7,914,147 B2.
5. Holz F.G., Schmitz-Valckenberg S., Spaide R.F., Bird A.C. Autofluorescence imaging. – Berlin, Heidelberg: Springer-Verlag, 2007. – P. 342. doi: 10.1007/978-3-540-71994-6.
6. Holz F.G., Schutt F., Kopotz J. Inhibition of lysosomal degradative functions in RPE cells by a retinoid component of lipofuscin // Invest. Ophthalmol. Vis. Sci. – 1999. – Vol. 40. – P. 737. PMID: 10067978.
7. Eldred G.E., Lasky M.R. Retinal age pigments generated by self-assembling lysosomotropic detergents // Nature. – 1993. – Vol. 361. – P. 724. doi: 10.1038/361724a0.
8. Von Ruckmann A., Fitzke F.W., Bird A.C. In vivo fundus autofluorescence in macular dystrophies // Arch. Ophthalmol. – 1997. – Vol. 115. – P. 609–615. doi: 10.1001/archopht.1997.01100150611006.
9. Boulton M., Dontsov A., Jarvis-Evans J., Ostrovsky M., Svistunenko D. Lipofuscin is a photoinducible free radical generator // J. Photochem. Photobiol. B: Biol. – 1993. – Vol. 19. – P. 201–204. doi: 10.1016/1011-1344(93)07173-3.
10. Yakovleva M.A., Feldman T.B., Krupennikova A.S., Borzenok S.A., Ostrovsky M.A. Fluorofory lipofuscinovych granul, otvetstvennie za autofluorescenciyu glaznogo dna cheloveka // Izvestiya Akademii Nauk. Seriya Khimicheskaya. – 2010. – No. 12. – P. 2252–2260.
11. Sparrow J.R., Vollmer-Snarr H.R., Zhou J. et al. A2E-epoxides damage DNA in retinal pigment epithelial cells. Vitamin E and other antioxidants inhibit A2E-epoxide formation // J. Biol. Chem. – 2003. – Vol. 278, No. 20. – P. 18207–18213. doi: 10.1074/jbc.M300155200.

12. Feldman T.B., Yakovleva M.A., Arbukhanova P.M., Borzenok S.A., Kononikhin A.S., Popov I.A. et al. Changes in spectral properties and composition of lipofuscin fluorophores from human retinal pigment epithelium with age and pathology. *Anal. Bioanal. Chem*., 2015, vol. 407, pp. 1075–1088. doi: 10.1007/s00216-014-8366-9.
13. Feldman T.B., Yakovleva M.A., Larichev A.V., Arbukhanova P.M., Radchenko A.Sh., Borzenok S.A., Kuzmin V.A., Ostrovsky M.A. Spectral analysis of fundus autofluorescence pattern as a tool to detect early stages of degeneration in the retina and retinal pigment epithelium. *Eye*, 2018, vol. 32, no. 9, pp. 1440–1448. doi: 10.1038/s41433-018-0090-7.
14. Bourauel L., Vaisband M., von der Emde L. et al. Spectral analysis of human retinal pigment epithelium cells in healthy and AMD eyes. *Invest. Ophthalmol. Vis. Sci*., 2024, vol. 65, pp. 10. doi: 10.1167/iovs.65.1.10.
15. Yakovleva M.A., Radchenko A.Sh., Feldman T.B., Kostyukov A.A., Arbukhanova P.M., Borzenok S.A., Kuzmin V.A., Ostrovsky M.A. Fluorescence characteristics of lipofuscin fluorophores from human retinal pigment epithelium. *Photochem. Photobiol. Sci*., 2020, vol. 19, no. 7, pp. 920–930. doi: 10.1039/C9PP00406H.
16. Schweitzer D., Quick S., Schenke S. et al. Comparison of parameters of time resolved autofluorescence between healthy subjects and patients suffering from early AMD. *Ophthalmologe*, 2009, vol. 106, pp. 714–722. doi: 10.1007/s00347-009-1975-4.
17. Sauer L., Gensure R.H., Andersen K.M., Kreilkamp K.M., Hageman G.S., Hammer M., Bernstein P.S. Patterns of fundus autofluorescence lifetimes in eyes of individuals with non-exudative age-related macular degeneration. *Invest. Ophthalmol. Vis. Sci*., 2018, vol. 59, pp. AMD65. doi: 10.1167/iovs.17-23764.
18. Pawley J. (ed.). Handbook of biological confocal microscopy. *3rd ed. Springer*, 2006. doi: 10.1007/978-0-387-45524-2.
19. Philip J.P., Carlsson K. Theoretical investigation of the signal-to-noise ratio in fluorescence lifetime imaging. *J. Opt. Soc. Am. A*, 2003, vol. 20, pp. 368–379. doi: 10.1364/JOSAA.20.000368.
20. Becker W. Fluorescence lifetime imaging — techniques and applications. *J. Microsc*., 2012, vol. 247, iss. 2, pp. 119–136. doi: 10.1111/j.1365-2818.2012.03618.x.
21. Smirnov K., Divochiy A., Vakhtomin Y., Morozov P., Zolotov P., Antipov A., Seleznev V. NbN single photon detectors with saturated dependence of quantum efficiency. *Superconductor Scienceand Technology*, 2018, vol. 31, no. 3, pp. 035011. doi: 10.1088/1361-6668/aaa56a.
22. Shcheslavskiy V., Morozov P., Divochiy A., Vakhtomin Yu., Smirnov K., Becker W. Ultrafast time measurements by time-correlated single photon counting coupled with superconducting single photon detector. *Rev. Sci. Instrum*., 2016, vol. 87, pp. 053117. doi: 10.1063/1.4952963.
23. Wang S., Yin Z.-Q., He D.-Y., Chen W., Wang R.-Q., Ye P., Zhou Y., Fan-Yuan G.-J., Wang F.-X., Zhu Y.-G., Morozov P.V., Divochiy A.V., Zhou Z., Guo G.-C., Han Z.-F. Twin field quantum key distribution over 830 km fibre. *Nature Photonics*, 2022, vol. 16, pp. 154–161. doi: 10.1038/s41566-021-00928-2.
24. Dontsov A., Yakovleva M., Trofimova N., Sakina N., Gulin A., Aybush A., Gostev F., Vasin A., Feldman T., Ostrovsky M. Water-soluble products of photooxidative destruction of the bisretinoid A2E cause proteins modification in the dark. *Int. J. Mol. Sci*., 2022, vol. 23, no. 3, pp. 1534. doi: 10.3390/ijms23031534.
25. Docchio F., Boulton M., Cubeddu R., Ramponi R., Dayhaw-Barker P. Age-related changes in the fluorescence of melanin and lipofuscin granules of the retinal pigment epithelium: a time-resolved fluorescence spectroscopy study. *Photochemistry and Photobiology*, 1991, vol. 54, pp. 247–253. doi: 10.1111/j.1751-1097.1991.tb02013.x.
26. Semenov A.N., Maksimov E.G., Moysenovich A.M., Yakovleva M.A., Tsoraev G.V., Ramonova A.A., Shirshin E.A., Sluchanko N.N., Feldman T.B., Rubin A.B., Kirpichnikov M.P., Ostrovsky M.A. Protein-mediated carotenoid delivery suppresses the photoinducible oxidation of lipofuscin in retinal pigment epithelial cells. *Antioxidants*, 2023, vol. 12, no. 2, pp. 413. doi: 10.3390/antiox12020413.
27. Dysli C., Wolf S., Berezin M.Y., Sauer L., Hammer M., Zinkernagel M.S. Fluorescence lifetime imaging ophthalmoscopy. *Prog. Retin. Eye Res*., 2017, vol. 60, pp. 120–143. doi: 10.1016/j.preteyeres.2017.06.005.
28. Eldred G.E., Katz M.L. Fluorophores of the human retinal pigment epithelium: separation and spectral characterization. *Exp. Eye Res*., 1988, vol. 47, pp. 71–86. doi: 10.1016/0014-4835(88)90055-2.
29. Sparrow J.R., Wu Y., Kim C.Y., Zhou J. Phospholipid meets all-trans retinal: the making of RPE bisretinoids. *J. Lipid Res*., 2009, vol. 51, pp. 247–261. doi: 10.1194/jlr.R000687.
30. Miura Y., Bernstein P., Dysli C., Sauer L., Zinkernagel M. Fluorophores in the eye. In: Zinkernagel M., Dysli C. (eds). Fluorescence Lifetime Imaging Ophthalmoscopy. *Cham: Springer International Publishing*, 2019, pp. 35–48. doi: 10.1007/978-3-030-22878-1_7.
31. Sonntag S., Klein B., Brinkmann R., Grisanti S., Miura Y. Fluorescence lifetime imaging ophthalmoscopy of mouse models of age-related macular degeneration. *Transl. Vis. Sci. Technol*., 2024, vol. 13, pp. 24. doi: 10.1167/tvst.13.1.24.

12. Feldman T.B., Yakovleva M.A., Arbukhanova P.M., Borzenok S.A., Kononikhin A.S., Popov I.A. et al. Changes in spectral properties and composition of lipofuscin fluorophores from human retinal pigment epithelium with age and pathology // Anal. Bioanal. Chem. – 2015. – Vol. 407. – P. 1075–1088. doi: 10.1007/s00216-014-8366-9.
13. Feldman T.B., Yakovleva M.A., Larichev A.V., Arbukhanova P.M., Radchenko A.Sh., Borzenok S.A., Kuzmin V.A., Ostrovsky M.A. Spectral analysis of fundus autofluorescence pattern as a tool to detect early stages of degeneration in the retina and retinal pigment epithelium // Eye. – 2018. – Vol. 32, No. 9. – P. 1440–1448. doi: 10.1038/s41433-018-0090-7.
14. Bourauel L., Vaisband M., Von der Emde L. et al. Spectral analysis of human retinal pigment epithelium cells in healthy and AMD eyes // Invest. Ophthalmol. Vis. Sci. – 2024. – Vol. 65. – P. 10. doi: 10.1167/iovs.65.1.10.
15. Yakovleva M.A., Radchenko A.Sh., Feldman T.B., Kostyukov A.A., Arbukhanova P.M., Borzenok S.A., Kuzmin V.A., Ostrovsky M.A. Fluorescence characteristics of lipofuscin fluorophores from human retinal pigment epithelium // Photochem. Photobiol. Sci. – 2020. – Vol. 19, No. 7. – P. 920–930. doi: 10.1039/C9PP00406H.
16. Schweitzer D., Quick S., Schenke S., Klemm M., Gehlert S., Hammer M., Jentsch S., Fischer J. Comparison of parameters of time-resolved autofluorescence between healthy subjects and patients suffering from early AMD // Ophthalmologe. – 2009. – Vol. 106. – P. 714–722. doi: 10.1007/s00347-009-1975-4.
17. Sauer L., Gensure R.H., Andersen K.M., Kreilkamp K.M., Hageman G.S., Hammer M., Bernstein P.S. Patterns of fundus autofluorescence lifetimes in eyes of individuals with non-exudative age-related macular degeneration // Invest. Ophthalmol. Vis. Sci. – 2018. – Vol. 59. – P. AMD65. doi: 10.1167/iovs.17-23764.
18. Pawley J. (ed.). Handbook of biological confocal microscopy. 3rd. ed. – Springer, 2006. doi: 10.1007/978-0-387-45524-2.
19. Philip J.P., Carlsson K. Theoretical investigation of the signal-to-noise ratio in fluorescence lifetime imaging // J. Opt. Soc. Am. A. – 2003. – Vol. 20. – P. 368–379. doi: 10.1364/JOSAA.20.000368.
20. Becker W. Fluorescence lifetime imaging — techniques and applications // Vol. 247, Is. 2. – 2012. – P. 119–136. doi: 10.1111/j.1365-2818.2012.03618.x.
21. Smirnov K., Divochiy A., Vakhtomin Y., Morozov P., Zolotov P., Antipov A., Seleznev V. NbN single-photon detectors with saturated dependence of quantum efficiency // Superconductor Science and Technology. – 2018. – Vol. 31, No. 3. – P. 035011. doi: 10.1088/1361-6668/aaa56a.
22. Shcheslavskiy V., Morozov P., Divochiy A., Vakhtomin Yu., Smirnov K., Becker W. Ultrafast time measurements by time-correlated single photon counting coupled with superconducting single photon detector // Rev. Sci. Instrum. – 2016. – Vol. 87.– P. 053117. doi: 10.1063/1.4952963.
23. Wang S., Yin Z.-Q., He D.-Y., Chen W., Wang R.-Q., Ye P., Zhou Y., Fan-Yuan G.-J., Wang F.-X.. Zhu Y.-G., Morozov P.V., Divochiy A.V., Zhou Z., Guo G.-C., Han Z.-F. Twin-field quantum key distribution over 830-km fibre // Nature Photonics. – 2022. – Vol. 16. – P. 154–161. doi: 10.1038/s41566-021-00928-2.
24. Dontsov A., Yakovleva M., Trofimova N., Sakina N., Gulin A., Aybush A., Gostev F., Vasin A., Feldman T., Ostrovsky M. Water-soluble products of photooxidative destruction of the bisretinoid A2E cause proteins modification in the dark // Int. J. Mol. Sci. – 2022. – Vol. 23, No. 3. – P. 1534. doi: 10.3390/ijms23031534.
25. Docchio F., Boulton M., Cubeddu R., Ramponi R., Dayhaw-Barker P. Age-related changes in the fluorescence of melanin and lipofuscin granules of the retinal pigment epithelium: a time-resolved fluorescence spectroscopy study // Photochemistry and Photobiology. – 1991. – Vol. 54. – P. 247–253. doi: 10.1111/j.1751-1097.1991.tb02013.x.
26. Semenov A.N., Maksimov E.G., Moysenovich A.M., Yakovleva M.A., Tsoraev G.V., Ramonova A.A., Shirshin E.A., Sluchanko N.N., Feldman T.B., Rubin A.B., Kirpichnikov M.P., Ostrovsky M.A. Protein-mediated carotenoid delivery suppresses the photoinducible oxidation of lipofuscin in retinal pigment epithelial cells // Antioxidants. – 2023. – Vol. 12, No. 2. – P. 413. doi: 10.3390/antiox12020413.
27. Dysli C., Wolf S., Berezin M.Y., Sauer L., Hammer M., Zinkernagel M.S. Fluorescence lifetime imaging ophthalmoscopy // Prog. Retin. Eye Res. – 2017. – Vol. 60. – P. 120–143. doi: 10.1016/j.preteyeres.2017.06.005.
28. Eldred G.E., Katz M.L. Fluorophores of the human retinal pigment epithelium: separation and spectral characterization // Exp. Eye Res. – 1988. – Vol. 47. – P. 71–86. doi: 10.1016/0014-4835(88)90055-2.
29. Sparrow J.R., Wu Y., Kim C.Y., Zhou J. Phospholipid meets all-trans retinal: the making of RPE bisretinoids // J. Lipid Res. – 2009. – Vol. 51. – P. 247–261. doi: 10.1194/jlr.R000687.
30. Miura Y., Bernstein P., Dysli C., Sauer L., Zinkernagel M. Fluorophores in the eye // In: Zinkernagel M., Dysli C. (eds). Fluorescence Lifetime Imaging Ophthalmoscopy. – Cham: Springer International Publishing, 2019. – P. 35–48. doi: 10.1007/978-3-030-22878-1_7.
31. Sonntag S., Klein B., Brinkmann R., Grisanti S., Miura Y. Fluorescence lifetime imaging ophthalmoscopy of mouse models of age-related macular degeneration // Transl. Vis. Sci. Technol. – 2024. – Vol. 13. – P. 24. doi: 10.1167/tvst.13.1.24.